CEAS Space Journal manuscript No.
(will be inserted by the editor)

Multiple Beacons for Supporting Lunar Landing Navigation

Stephan Theil · Leonardo Bora

Received: date / Accepted: date

Abstract The exploration and potential future exploitation of solar system bodies requires technologies for precise and safe landings. Current navigation systems for landing probes are relying on a combination of inertial and optical sensor measurements to determine the current flight state with respect to the target body and the desired landing site. With a future transition from single exploration missions to more frequent first exploration and then exploitation missions the implementation and operation of these missions changes since it can be expected that a ground infrastructure on the target body is available in the vicinity of the landing site. In a previous paper the impact of a single ground-based beacon on the navigation performance was investigated depending on the type of radiometric measurements and on the location of the beacon with respect to the landing site. This paper extends this investigation on options for ground-based multiple beacons supporting the on-board navigation system. It analyses the impact on the achievable navigation accuracy. For that purpose the paper introduces briefly the existing navigation architecture based on optical navigation and its extension with radiometric measurements. The same scenario of lunar landing as in the previous paper is simulated. The results are analysed and discussed. They show a single beacon at a large distance along the landing trajectory and multiple beacons close to the landing site can improve the navigation performance. The results show how large the landing

S. Theil
German Aerospace Center (DLR)
Institute of Space Systems, GNC Systems Department
Tel.: +49-421-24420-1113
Fax: +49-421-24420-1120
E-mail: stephan.theil@dlr.de

L. Bora
AIRBUS Defence & Space Ltd
Tel.: +44-1438-77-4186
E-mail: leonardo.bora@airbus.com

area can be increased where a sufficient navigation performance is achieved using the beacons.

Keywords lunar landing · autonomous navigation · beacon navigation

1 Introduction

Safe and soft landing on a celestial body (planet, moon, asteroid, comet) has been a central objective for space exploration. Current navigation systems have achieved an large improvement in accuracy and safety compared to the first system e.g. from the Apollo era. This has been achieved by applying new sensor technologies and new filtering techniques.

In the future more exploration missions will land on the same celestial bodies. Therefore more resources on the ground can be made available for the following missions. First implementations of co-located ground infrastructure are probably robotic lunar bases which will be followed by a human base. Both scenarios (robotic or manned lunar base) serve as a motivation to investigate the impact of ground infrastructure providing radiometric measurement to the navigation system of later arriving landing and potentially also departing vehicles.

This paper continues the analysis of the impact of radio beacons on the lunar surface which was started in the previous paper [9]. The previous analysis started from a baseline navigation system with current technologies and analysed the improvement of the navigation solution when using a single beacon on ground located close to the landing site. The current paper uses information from this reference which is partly repeated for sake of completeness and the logic of the paper. However, more detailed information and justifications can be found in the above mentioned reference. The following information have been inherited from the reference above. For a detailed discussion and justification of these items we refer to the referenced paper.

- Navigation system architecture,
- Measurement models for laser altimeter and radiometric measurements,
- Landing scenario and trajectory for a lunar landing,
- Performance evaluation functions,
- Error models and parameters for all sensors,
- Reference navigation solution without support from beacon radiometric measurements, and
- Position of single beacon wrt. landing site with best performance.

This paper starts in section 2 with a short introduction of the state-of-the-art navigation system architecture for planetary landers and its extension using radiometric measurements from ground based infrastructure.

Section 3 introduces the lunar landing scenario used as a reference mission which will be utilized again for the analysis of the effect of multiple beacons. The navigation requirements for landing vehicles and the definition of evaluation functions are given.

In section 4 the simulation results are analysed. The first question to be answered is: How can beacons be optimally placed on larger distances to the landing site along the trajectory? Furthermore different configurations of multiple beacons are analysed to answer the question: Is it useful to place multiple beacons close to the landing site? And, what is the configuration of multiple beacons close to the landing site providing the best navigation performance?

Finally, the results from all test cases are discussed and a recommendation for a beacon configuration is given.

2 Navigation System and Filter Design

2.1 Navigation System Architecture

The following baseline navigation system architecture has been extended with radiometric measurements of beacon signals. The inputs used by the navigation system are sensor measurements and image processing results from:

- an Inertial Measurement Unit (IMU),
- a star tracker (ST),
- a laser altimeter (LA),
- a feature tracking algorithm (FT) providing feauture positions in the camera frame, and
- a crater navigation algorithm (CN) providing absolute position measurements,

where the results of feature tracking and crater navigation are obtained from processing images taken by a navigation camera.

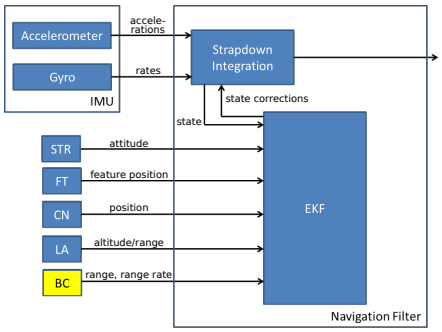

Fig. 1 Functional block diagram of the navigation system with beacons. The measurement from beacons is highlighted in yellow. The measurements from multiple beacons are denoted here in a single block.

The inputs to the navigation filter are extended with radiometric measurements from received beacon signals as shown in figure 1. The navigation filter is a discrete delayed error-state EKF (eEKF), which copes with the fact that

measurements in the real system are not instantly available but with delays (all but the ones from the IMU) (see [8]). The state vector is defined as

$$\mathbf{x} = \left\{ \begin{array}{c} \mathbf{r}^{MCMF} \\ \mathbf{v}^{MCMF} \\ \boldsymbol{\theta}^{B} \\ \mathbf{b}_{a}^{B} \\ \mathbf{s}_{a}^{B} \\ \mathbf{b}_{g}^{B} \\ \mathbf{s}_{g}^{B} \\ \boldsymbol{\xi}_{i}^{MCMF} \end{array} \right\} \tag{1}$$

where $\mathbf{r}^{MCMF}$ and $\mathbf{v}^{MCMF}$ denote position and velocity in Moon Centered Moon Fixed Frame (MCMF)[1]. $\boldsymbol{\theta}^{B}$ are attitude error angles. $\mathbf{b}_{a}^{B}$, $\mathbf{s}_{a}^{B}$, $\mathbf{b}_{g}^{B}$, and $\mathbf{s}_{g}^{B}$ are the accelerometer and gyro biases and scale factors. The additional states $\boldsymbol{\xi}_{i}^{MCMF}$, are the tracked feature positions with $i = 1..N$ and N as the number of features. They are necessary for the terrain relative navigation, which are feature positions needed to build the terrain model which is estimated through the solution of the simultaneous localization and mapping (SLAM) problem as proposed in [3].

The measurement models used to update the error states are based on the developments in [5,8,3]. For the update by the laser altimeter measurements a modification was introduced which is exploiting the fact that the vehicle is landing at a well determined landing site, whose topographic elevation is known a priori.

2.2 RF Measurement Models

As additional inputs for the navigation filter update the following three types of radiometric measurements of beacon signals have been introduced:

- range measurement (ρ),
- range rate measurement ($\dot{\rho}$).

The models are summarized here for sake of completeness.

2.2.1 Range

The range is the measurement of the distance between the beacon and the antenna on board of the spacecraft (see figure 2).

The range vector between the beacon (BC) and the receiver is

$$\boldsymbol{\rho}^{PCPF} = \mathbf{r}_{SC}^{PCPF} - \mathbf{r}_{BC}^{PCPF} \tag{2}$$

[1] with the origin in the center of the Moon, z-axis pointing to the North pole, and x- and y-axes spanning the equatorial plane.

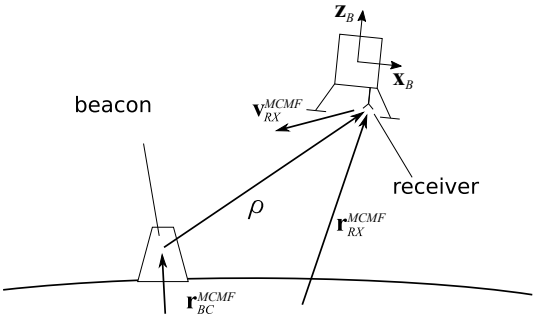

Fig. 2 Representation of range measurement between spacecraft and beacon on lunar surface

$$\boldsymbol{\rho} = \mathbf{r}_{RX} - \mathbf{r}_{BC} = \mathbf{r} + \mathbf{R}_B^{MCMF}\, \boldsymbol{\ell}_{RX}^B - \mathbf{r}_{BC} \tag{3}$$

where $\boldsymbol{\ell}_{RX}^B$ is the lever arm of the receiver with respect to the IMU (defined in the navigation body frame). Since in this study the clock bias is accounted as a random error, the pseudorange and range are equal and can be expressed as

$$\rho = \rho(\mathbf{r}_{SC}^{PCPF}) = \|\boldsymbol{\rho}^{PCPF}\| + w_\rho \tag{4}$$

with w_ρ as the range measurement noise.

2.2.2 Range-Rate

The range-rate is the relative velocity between the on-board receiver and the beacon in the range direction. Then the observation equation is

$$\dot{\rho} = \dot{\rho}(\mathbf{r}, \mathbf{v}, \boldsymbol{\theta}^B, \mathbf{b}_g^B, \mathbf{s}_g^B) = -\mathbf{v}_{RX}^T\, \frac{\boldsymbol{\rho}}{\rho} + w_{\dot{\rho}} \tag{5}$$

$$\dot{\rho} = \dot{\rho}(\mathbf{r}_{SC}^{PCPF}, \mathbf{v}_{SC}^{PCPF}) = \mathbf{v}_{SC}^{PCPF^T}\, \frac{\boldsymbol{\rho}}{\rho} + w_{\dot{\rho}} \tag{6}$$

where the velocity of the receiver in MCMF frame is

$$\mathbf{v}_{RX} = \mathbf{v} + (\mathbf{R}_B^{MCMF}[\boldsymbol{\omega}_{I,B}^B\times] - [\boldsymbol{\omega}_{I,M}^M\times]\mathbf{R}_B^{MCMF})\, \boldsymbol{\ell}_{RX}^B. \tag{7}$$

2.2.3 Visibility Model

The measurements of the beacon will be only available if the lander is visible. Figure 3 sketches the condition for the visibility. Since the real morphology of the surface is unknown and not taken into account in this analyis, a minimum elevation angle of $\beta_{LIM} = 10deg$ with respect to the local horizon is set to consider the lander visible from the beacon. Only in this condition the measurement is treated as valid and is used to update the navigation state.

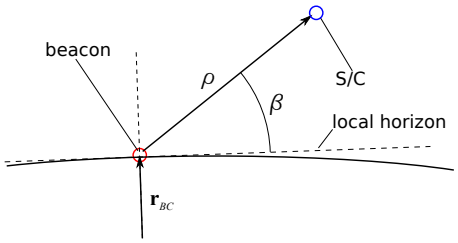

Fig. 3 Visibility model

3 Scenario and Analyses Method

3.1 Definition of Lunar Landing Scenario

The scenario is a lunar soft landing starting with a maneuver for descent orbit injection from a 100x100 km polar orbit. At perigee the powered descent is initiated. At an altitude of 2 km High Gate is reached where final landing phase starts. Finally, a vertical descent is performed from around 1 km altitude.

During powered descent the attitude of the lander is constrained by the thrust profile. The antenna used to receive the beacon signals is attached near the navigation camera on the bottom surface of the lander that it is directly visible from the beacons.

The simulation starts with the descent orbit burn and ends at an altitude of 1 m above the landings site. So it includes all parts of the landing except touch down. The final velocity is less than 0.5 m/s. For later analyses it is useful to show the powered descent groundtrack on the local horizontal plane, in order to better understand some considerations during the analyses (figure 4(right)).

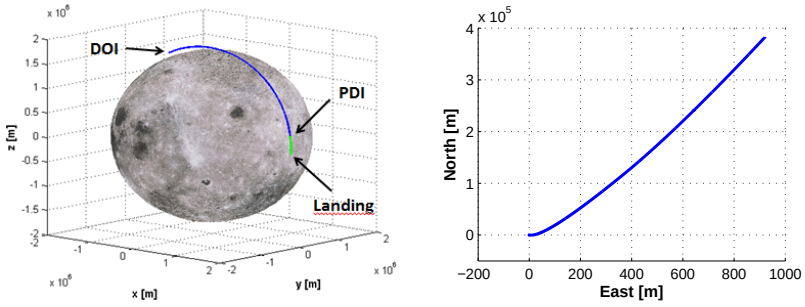

Fig. 4 Landing trajectory (left) and groundtrack of final phase in local horizontal plane (right); DOI - Descent Orbit Injection; PDI - Powered Descent Initiate

3.2 Simulation Set-up

The results presented in this paper have been generated with Monte Carlo analyses with 100 runs. In each run the initial navigation error, the random seeds for all noise generators as well as the systematic errors of the sensors (e.g. bias, scale factor) have been randomly changed. All other parameters like vehicle parameters, environment and trajectory have not been changed.

After the Monte Carlo simulation for each set-up, 100 navigation solutions are available. From this data set a worst case navigation solution is extracted as the maximum absolute navigation error per each time instant i of the navigation solution for all runs N_{MC}. The worst case error ΔE_i can be written as

$$\Delta E_i = max(|\Delta e_{i,j}|)_{j=1}^{N_{MC}} \tag{8}$$

where $\Delta e_{i,j}$ is the error between the result of the navigation solution of Monte Carlo run j at a given time instant i and the true state at the same time.

The output of each Monte Carlo analysis for a given beacon configuration under study, is processed through equation (7). Similarly, the baseline worst case solution without beacon has been obtained. It serves as the reference for comparing the different beacon configurations.

3.3 Error Models

This section defines the error models for the measurements in the navigation system.

Table 1 lists the parameters for the Inertial Measurement Unit (IMU) used in the simulations. In table 2 the noise figures associated to the rest of the baseline sensor suite are shown.

In table 3 the noise figures associated to the measurements from the beacons are shown.

3.4 Navigation Requirements and Evaluation Method

3.4.1 Navigation Accuracy Requirement Profile

For the trade-offs presented in this paper the same definition of an evaluation function is used as defined in [9]. It is based on relevant lunar landing requirements from [4,6,10,2]. The values in detail can be seen in table 4. They are given in downrange (DR), crossrange (CR), and altitude (A). The three directions form the DCA[2] frame. The same coordinates will be used for the analysis of results later in this paper.

[2] where the downrange direction points in nominal flight direction, altitude is aligned along the local vertical and crossrange is perpendicular to both.

Table 1 IMU parameters (1-σ)

Parameter	Value	Units
Accelerometer		
- Bias level	25.5	mg
- Bias stability	1.5	mg
- Random walk	0.0106	m/s/$\sqrt{hr}$
- Scale factor error	$3.33 \cdot 10^{-4}$	-
- Scale factor error stability	$1.67 \cdot 10^{-6}$	-
Gyroscope		
- Bias level	825	deg/hr
- Bias stability	4	deg/hr
- Random walk	0.9	deg/$\sqrt{hr}$
- Scale factor error	$3.33 \cdot 10^{-5}$	-
- Scale factor error stability	10^{-6}	-

Table 2 Error parameters (1-σ) for star tracker (STR), crater navigation (CN), feature tracker (FT) and laser altimeter (LA).

Parameter	Value	Units
STR accuracy	9.1	arcsec
CN accuracy	3 % of slant-range	m
FT accuracy	1	pixel
LA accuracy	0.04	m

Table 3 Beacon measurements error parameters (1-σ)

Parameter	Value	Units
Range	10	m
Range-rate	0.1	m/s

Table 4 3-σ navigation accuracy requirement from Powered Descent Initiate (PDI), through High Gate (HG) to landing; DR - downrange; CR - crossrange; A - altitude

	PDI		**HG**		**Landing**	
	$\Delta\bar{E}_r[m]$	$\Delta\bar{E}_v[m/s]$	$\Delta\bar{E}_r[m]$	$\Delta\bar{E}_v[m/s]$	$\Delta\bar{E}_r[m]$	$\Delta\bar{E}_v[m/s]$
DR	2000	1	100	0.5	10	0.1
CR	2000	1	100	0.5	10	0.1
A	200	1	20	0.5	0.5	0.1

Based on the requirements in table 4 the derived profiles for the navigation accuracy requirements are shown in figure 5. This study focuses on the navigation performance in the most critical phase the powered descent. Therefore the profiles start at PDI.

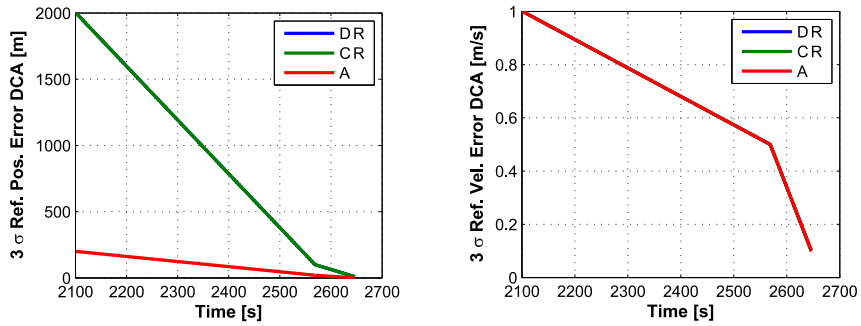

Fig. 5 Navigation accuracy requirement profiles

3.4.2 Evaluation Functions

The general form of the evaluation functions is

$$J = \frac{1}{N} \sum_{i=I_0}^{I_F} \left(\frac{\Delta E_i}{\Delta \bar{E}_i} \right)^2 \tag{9}$$

where $\Delta \bar{E}_i$ is the 3-σ navigation accuracy requirement corresponding to the assessed navigation error; i is the index for the time of the navigation solutions; I_0 and I_F are respectively the initial and final time indexes corresponding to the time interval in which the evaluation function has to be evaluated; N is the number of samples in the interval.

Equation (8) is basically similar to an integral of the worst case navigation solution errors (equation (7)) weighted with the navigation accuracy requirements $\Delta \bar{E}_i$ defined in the previous subsection.

A number of four intervals has been defined, in which these functions are evaluated. The main interval goes from a defined start time (called t_{start}) to the landing (evaluation function class J). This interval is meant to study the performance for the whole period in which the beacon measurements have an impact on the navigation solution.

The other three are sub-intervals of the main. They are needed in order to allow a more detailed evaluation of the performance of a given configuration. This way it is possible to see how the studied option impacts on the different relevant phases of the landing. The three subintervals are:

1. The interval corresponding to evaluation function class J_1 starts at t_{start} and ends at t_{MID}, which is defined as the mid point between t_{start} and t_{HG}, i.e. the time in which the S/C reaches High Gate.
2. The interval for J_2 starts at t_{MID} and ends at t_{HG}.
3. The interval related to J_3 goes from t_{HG} to the landing at t_{final}.

In total, 24 independent evaluation functions are available. In table 5 a notation overview is shown for the evaluation function class J_1, in order to make the reader to understand the notation used in the analysis.

Before discussing the results it should be noted that a value of the evaluation function above 1 indicates that the analysed configuration is performing worse than the requirements. If the evaluation function value is below 1 the requirements are met on average.

Table 5 Evaluation function notation (example for J_1)

	DR	CR	A	Total
Position	$J_{1,r}^{DR}$	$J_{1,r}^{CR}$	$J_{1,r}^{A}$	$J_{1,r}^{tot} = J_{1,r}^{DR} + J_{1,r}^{CR} + J_{1,r}^{A}$
Velocity	$J_{1,v}^{DR}$	$J_{1,v}^{CR}$	$J_{1,v}^{A}$	$J_{1,v}^{tot} = J_{1,v}^{DR} + J_{1,v}^{CR} + J_{1,v}^{A}$

4 Simulation Results and Analysis

4.1 Baseline Navigation Solution

In order to be able to assess the results from the analysis of multiple beacons the baseline worst case navigation solution is presented. Table 6 shows the values for the cost functions when the start of the evaluation time interval t_{Start} is equal to the time of first visibility of a beacon located at the landing site. In later analysis these reference values may change if the value of t_{Start} is changed.

Table 6 Evaluation function values for baseline scenario (without beacons)

	Symbol	J_1	J_2	J_3	J
Position	$J_{i,r}^{DR}$	0.08	0.26	12.94	3.33
	$J_{i,r}^{CR}$	0.01	0.12	10.68	2.69
	$J_{i,r}^{A}$	3.53	5.81	6.46	5.11
	$J_{i,r}^{tot}$	3.63	6.21	30.09	11.14
Velocity	$J_{i,v}^{DR}$	7.27	0.65	0.13	3.02
	$J_{i,v}^{CR}$	0.57	0.10	0.04	0.26
	$J_{i,v}^{A}$	2.80	0.28	0.46	1.28
	$J_{i,v}^{tot}$	10.66	1.04	0.65	4.57

4.2 Impact of a Single Beacon on Different Landing Phases

In [9] the placement of a single beacon close to the landing site was analysed. In this analysis the position of the beacon was varied in a square of 20 km centered around the landing site. The analysis showed that this had the largest impact on landing accuracy since the radiometric measurements from the beacon signal provided high accuracy close to the landing site where it is needed.

With the idea of placing several beacons on the ground the question arises if it is useful to place more beacons close to the landing site or along the approach to the landing site.

For that purpose the analysis for a single beacon has been extended to a larger area around the landing site. It is 60 km in East-West direction centered on the landing site. In North-South direction it extends over 200 km from 50 km South to 150 km North of the landing site. Since the approach is almost straight from North, beacons located far North will still have an impact on the navigation accuracy although they are not visible for the last phase of the landing.

In order to compare the results of all beacon locations and their impact on the different phases of the landing, the time periods as described in section 3.4.2 are defined with the values in table 7. The beginning of this time line is on the descent orbit after a correction manoeuvre. The powered descent starts at $t_{PD} = 2100\,s$. The time t_{start} was chosen since this is the earliest visibility of a beacon located 150 km North of the landing site.

Table 7 Time intervals for analysis of landing phases

t_{start}	t_{MID}	t_{HG}	t_{final}
2210 s	2390 s	2569 s	2646.4 s

In figure 6(left) the evaluation function for the position J_r^{tot} is plotted as a contour plot showing its dependency on the beacon location. From these results a few points can be concluded: For beacons South of the landing site the visibility is reduced the more South they are located. The result is that they have almost no impact on the accuracy. For all beacons from 20 km South of the landing site to the North the navigation solution accuracy is improved. This shows that even in cases where the beacon is only visible during a short time during the approach but where it is not visible in the last phase of the landing, the overall accuracy is better than in the baseline configuration without radiometric measurements.

In figure 6(right) a similar behaviour can be observed for the navigation accuracy in the last phase (interval 3) and its corresponding evaluation function $J_{3,r}^{tot}$. It shows that an early correction with radiometric measurements from the beacon supports the navigation accuracy to a large extend. It does not help to achieve values of the evaluation function $J_{3,r}^{tot}$ below 1 but it reduces the evaluation function values significantly to less than a third with respect to the baseline configuration without beacons.

Figure 7 shows the evaluation functions for the navigation accuracy in the first two phases until High Gate. From figure 7(left) it can be seen that the first interval between t_{start} and t_{MID} the best improvement is achieved with beacons located under the flight path of the landing vehicle.

Similarly, the accuracy is improved in the second interval between t_{MID} and t_{HG} if the beacon is positioned below the trajectory (see figure 7(right)).

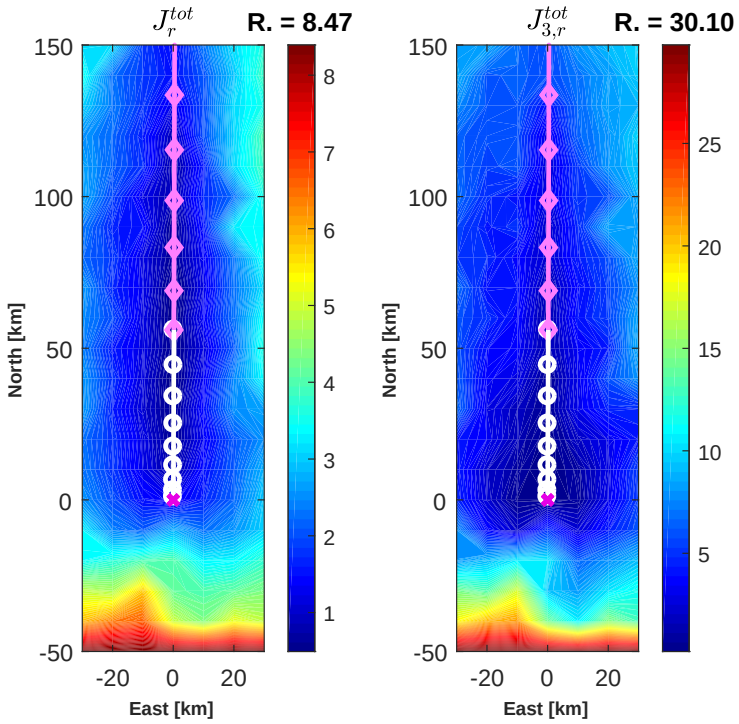

Fig. 6 Position evaluation functions for a single beacon: J_r^{tot} (left), $J_{3,r}^{tot}$ (right). The landing trajectory is fixed to the map. The color shows the evaluation function for a beacon at this location. The value above each color bar shows the same cost function value for the baseline case without RF measurements. The lines with markers denote the ground track: pink with diamonds for interval 1, white with circles interval 2 and purple for interval 3. Each marker denotes a time distance of 20 s.

For the second interval lower evaluation functions values are also achieved if the beacon is located far North with low visibility. This again confirms that a high navigation accuracy achieved in the early phase of the landing can be propagated to later phases.

From these results it can be concluded that a beacon located about 50 to 70 km North of the landing site would improve the navigation accuracy until High Gate to a level that the evaluation functions for both intervals 1 and 2 are below 1 indicating that the requirements for both phases are fully met. The navigation accuracy in the third interval would be also improved with respect to the baseline set-up but the requirements would not be fully met for the positioning accuracy. Therefore, it can be concluded that at least one more beacon needs to be provided at the landing site.

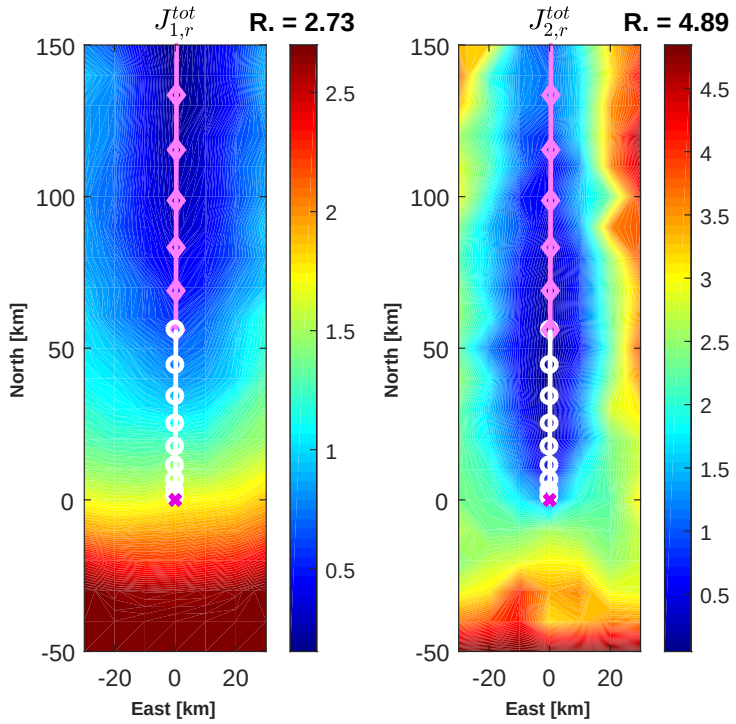

Fig. 7 Position evaluation functions for a single beacon: $J^{tot}_{1,r}$ (left), $J^{tot}_{2,r}$ (right). The landing trajectory is fixed to the map. The color shows the evaluation function for a beacon at this location. The value above each color bar shows the same cost function value for the baseline case without RF measurements. The lines with markers denote the ground track: pink with diamonds for interval 1, white with circles interval 2 and purple for interval 3. Each marker denotes a time distance of 20 s.

4.3 Multiple Beacons Close to the Landing Site

In the previous paper [9] a single beacon close to the landing site was analysed. It was shown that beacon positions can be found where the navigation accuracy requirements can be met with all evaluation function values below 1.0. This was possible with and without the bearing measurement of the beacon. The area where this can be achieved with a single beacon is small and very close to the landing site.

NASA recommended in [7] to avoid landing and flying closer than 2 km from objects on the surface to protect them. This would exclude an area around the beacon where a high navigation accuracy is provided. Illustrating this fact figure 8 shows in a contour plot the evaluation function for the position J^{tot}_r and the worst case final horizontal error ΔE_H for a single beacon providing range and range-rate measurements. Unlike the plots in the previous section these plots show the evaluation function and landing error values at the position where the landing occurs while the beacons are fixed to the map. In both

plots of figure 8 the position of the beacon is marked with a pink cross. It is the position which was proposed in [9] as the best solution for a single beacon and an intended landing at position (0,0) in the map. The avoidance area for the landing is shown as a pink circle. The area below this circle enclosed with a pink dashed line also has to be avoided if the landing vehicle shall not fly over the avoidance area (pink circle) when approaching roughly from North direction.

NASA's recommendation in [7] refers to the preservation of historic landing sites. It has been used as a reference for this paper. However, for future operational hardware shorter distances between landing site and beacons can be allowed. Determining the minimum allowed distance is subject to detailed analysis or mitigation measures, e.g. potential preparation of the landing site with a solid landing pad or walls of regolith around the landing site to shelter .

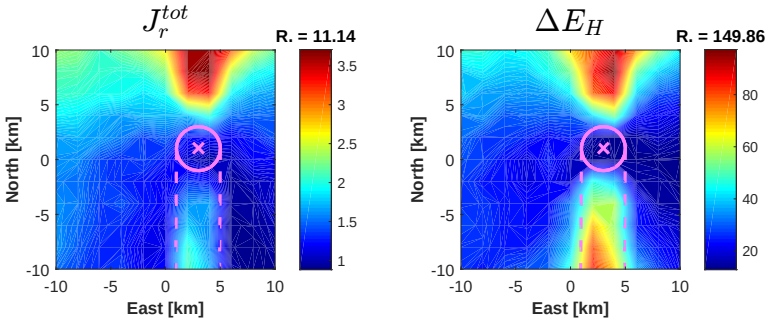

Fig. 8 Position evaluation functions for a single beacon: Evaluation function J_r^{tot} (left), worst case horizontal landing error ΔE_H (right). Beacons are fixed to the map. The color shows the evaluation function for a landing at this location. The value above each color bar shows the same cost function value for the baseline case without RF measurements. The pink crosses denote the beacon positions. The pink circle represent areas where a landing is not possible (closer than 2 km to the beacon). The pink dashed lines enclose the area where a landing is not possible without flying over the area closer than 2 km to the beacon.

Since the goal is to enable landings of several spacecraft from the same approach direction (North to South) with beacons as ground infrastructure, a large designated landing area with a high navigation accuracy is needed. This would increase the flexibility on the selection of the exact landing spot. Especially, if each new arriving vehicle could create a new no-landing and no-fly-over zone and avoidance area on ground.

Adding one or more beacons around the landing site would increase the area with sufficient navigation accuracy. This would also increase the failure tolerance by adding a redundancy to the system. From this conclusion the following questions arise: How many beacons are needed? How shall the beacons be positioned with respect to the targeted landing zone?

Starting from the results in figure 8 up to three beacons are added in a symmetric configuration until a square configuration of 6 km by 6 km with four beacons is created. There are six combinations for selecting two beacons out of four. Three of these combinations with two beacons have been analysed in addition to the configurations with one, three and four beacons.

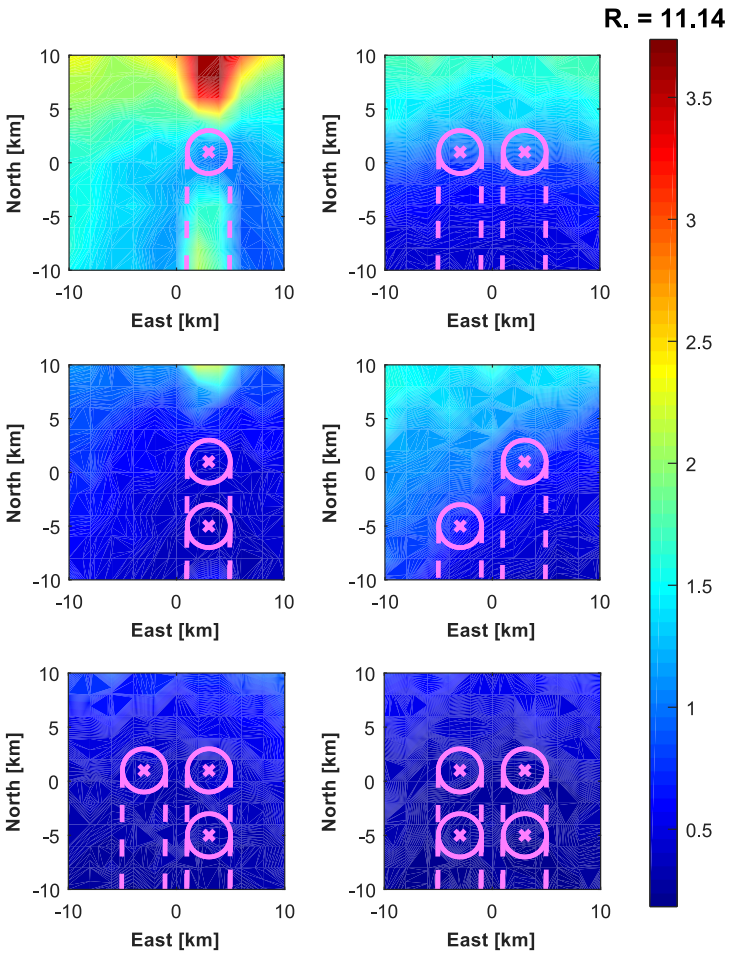

Fig. 9 Position evaluation function J_r^{tot} for different beacon configurations. Beacons are fixed to the map. The color shows the evaluation function for a landing at this location. The value above the color bar shows the same cost function value for the baseline case without RF measurements. The pink crosses denote the beacon positions. The pink crosses denote the beacon positions. The pink circle represent areas where a landing is not possible (closer than 2 km to the beacon). The pink dashed lines enclose the area where a landing is not possible without flying over the area closer than 2 km to the beacon.

Figure 9 shows the evaluation function for the position J_r^{tot} for six selected combinations with the same color scaling. It can be seen that as soon as a

second beacon is added the area with a total evaluation function J_r^{tot} below 1.0 increases dramatically. For the cases with three and four beacons the whole area of 10 km by 10 km has a value below 1.0. Based on these results one of the questions raised above could be partly answered: two or more beacons are needed to create a large area with sufficient navigation accuracy.

The second question regarding the positions of the beacons cannot be easily answered. The decision about where to put the beacons on ground is not solely determined by the navigation accuracy. As the avoidance areas in figure 9 show a large part of the area with good navigation performance during landing must be excluded depending on approach direction and location of the beacons. If the approach direction changes the distribution of the navigation performance and the avoidance areas also change. So, a very large impact on the optimal beacon positions comes from the operational concept which determines the number of landings as well as the approach directions. Furthermore, the effort needed to place the beacons must be part of the trade-off. Placing a large number of beacons separated by large distances in the order of several tens of kilometers would - of course - require much more efforts than distributing a small number in an area of only one kilometer in both directions. Since the optimal configuration is extremely mission dependent the following analysis provides a parametric variation of a few configurations to show the general impact on the navigation performance.

Based on the first analysis presented in figure 9 the following variations are introduced:

- The size of the analysed potential landing area is increased to a square of 40km by 40km (±20km in East-West and North-South directions) around a nominal landing point at coordinates (0,0).
- From the square pattern of beacon locations centered at the point (0,0) different beacons are selected. The locations are denoted as *A*, *B*, *C*, and *D* in figure 10.
- The size of the square pattern of beacons from which two, three or four beacons are selected is varied. Its edge length is varied from 1km to 20km to see if a large area for landings between the beacons can be created.
- The analysis of the different configurations computes the percentage of the whole 40km×40km area which fulfils the following conditions:
  1. The area that shall not be passed according to NASA's recommendations in [7]. The circular region around the beacon is denoted as no-landing zone. The area south of these circles is to be avoided if the vehicle shall not fly over the circular region around the beacon (no-landing/no-fly-over).
  2. The area where a landing is possible with a total evaluation function of $J_{r,tot} < 1$ excluding the no-landing zone.
  3. The area with a worst case horizontal position landing error of $\Delta E_{r,h} < 50m$ excluding the no-landing zone.
  4. The area with a worst case horizontal position landing error of $\Delta E_{r,h} < 10m$ excluding the no-landing zone.

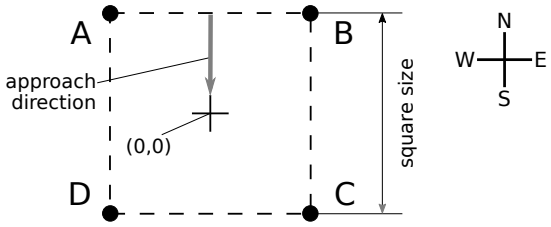

Fig. 10 Sketch of analysed beacon configurations including approach direction of landing trajectories

In order to estimate the areas a simplified approach is used. For computing the maps a grid of positions with 2km distance between the nodes in East-West and North-South direction has been computed as for the results in figures 8 and 9 above. In order to compute the area for each grid point the four conditions above are checked and the grid points are counted where the conditions are met. Thus the area ratio is computed as the ratio of the number of grid points wrt. the total number of grid points ($21 \times 21 = 441$). This simplified analysis is not applicable to a detailed analysis needed for a dedicated mission but it shows the general impact of varying the configuration.

It also has to be noted that for this analysis the topography of a smooth (spherical) Moon has been assumed. If applied to a mission the local topography has to be taken into account since it may have a large impact on beacon visibility and therefore on the navigation performance.

Table 8 shows the results of the analyses. For reference, the first line shows the results for a single beacon 500m North and 500m West of the nominal landings site at (0,0). From the results in the table many things can be observed:

- The more beacons are used the larger are the areas where the respective three conditions for successful landing are met. This is not surprising at all since more beacons can cover a larger area even if there is only one beacon visible that can be used for navigation. Secondly, in areas where multiple beacons can be used for navigation the performance is improved wrt. a single beacon.
- The larger the distance between the beacons is, the larger is the area with sufficient navigation performance. This can be expected since a large separation on ground creates for higher altitudes a better geometric condition for the navigation solution equal to the GDOP for GNSS navigation.
- If only two beacons as the minimal multi-beacon configuration are considered it can be seen that a separation along track provides a larger landing area with sufficient navigation performance. The reason is that for landings passing the two beacons along track the downrange components of the navigation state are optimally observable. Furthermore the observability of the crossrange components is improved at larger distances to the beacons via triangulation. It is worst when exactly flying over the two beacons, which is only theoretically useful since the two beacons could create a no-fly-over

Table 8 Results for different configurations of multiple beacons; the color coding of the cells ranges from red (0% of area ratio) via yellow (50% of area ratio) to green (100% of area ratio).

Size (km)	Number of beacons	Beacon IDs	No-land./ no-fly-over	Area ratio (%) $J_{r,tot} < 1$	$\Delta E_{r,h} < 50m$	$\Delta E_{r,h} < 10m$
1	1	A	1/5	2	66	0
1	2	AB	1/8	23	81	0
1	2	AD	1/5	11	70	0
1	3	ABD	1/8	28	85	1
1	4	ABCD	1/8	32	88	2
2	2	AB	1/8	33	91	2
2	2	AD	1/5	23	76	3
2	3	ABD	2/8	43	95	7
2	4	ABCD	2/8	52	98	9
4	2	AB	2/12	46	98	11
4	2	AD	2/6	53	87	11
4	3	ABD	3/12	68	97	27
4	4	ABCD	4/12	74	96	38
10	2	AB	2/13	58	98	50
10	2	AD	2/6	80	95	47
10	3	ABD	3/13	95	97	86
10	4	ABCD	4/13	96	96	95
20	2	AB	2/15	72	98	83
20	2	AD	2/8	78	94	76
20	3	ABD	3/16	97	97	94
20	4	ABCD	4/16	95	95	95

zone exactly where the navigation performance is worst. This marks a second positive result for two beacons in along-track configuration. Since the no-fly-over zones created by the two beacons overlap, the area with good navigation performance increases without reducing it due to no-fly-over zones.

– The square of four beacons with 20km edge length provides in the whole area of 40km×40km a navigation accuracy meeting the requirements of of $J_{r,tot} < 1$ and $\Delta E_{r,h} < 10m$. The area is only decreased by the no-landing and no-fly-over zones created by the beacons themselves. The coverage of the beacons goes even beyond the analysed area. This configuration would be probably the best option creating the largest area with landings supported by beacon navigation. It is also the most flexible in terms of alternative approach directions. An approach from North, East, South and West would render similar results. Approaches from other angles would reduce the accessible area due to larger no-landing or no-fly-over zones but would probably render similar navigation accuracy in a sufficiently large area.

Based on the results of this analysis a first recommendation can be given for a first stage of beacon deployment where only two beacons can be placed on ground. In this case the two beacons shall be placed around the intended landing sites separated along track with the largest possible distance (maxi-

mum 20km). This would be of course only a preliminary result since the final analysis for a mission must include the topography in order to avoid shadowing and to exploit optimal positions of the beacon on the hilltops surrounding the planned landing site.

5 Conclusions and Outlook

This paper presented a study on how the navigation for a lunar lander can be improved by using RF measurements from multiple ground-based beacons. For that purpose the navigaton filter of an existing navigation system based on IMU, image processing and laser altimeter was augmented to process range and range-rate measurements from the received multiple beacon signals. With this set-up an extensive Monte-Carlo simulation campaign was carried out in order to analyse the impact of the position of the beacons on the navigation solution.

For comparing the results of the different beacon locations evaluation functions have been defined which related the worst case error of the Monte-Carlo analysis to the requirements. For these evaluation functions contour plots were generated which show the dependency of the different evaluation functions on the position of the beacons.

For placing multiple beacons two different set-ups were analysed. First, the impact of a beacon was investigated which is placed close to the landing trajectory but far uprange to the landing site. From the results it can be concluded that a beacon located about 50 to 70km North of the landing site would improve the navigation accuracy until High Gate to a level that the requirements until High Gate are fully met. The navigation accuracy after High Gate until landing would then be also improved with respect to the baseline set-up since the improved navigation solution is propagated. But the requirements would not be fully met for the positioning accuracy at landing. Therefore it can be concluded that at least one more beacon needs to be provided at the landing site.

Secondly, up to four beacons located close to the intended landing site in different patterns where analysed. The best configuration with four beacons in a square with 20km edge length covers the whole analysed area of 40km$\times$40km providing a navigation accuracy meeting all requirements. The best trade-off is provided by only two beacons separated in along track direction by a large distance (e.g. 20km).

Based on these results in a next step it will be analysed how many beacons in what locations are needed to do a powered descent and landing without optical navigation. By enabling and disabling some of the sensor outputs an analysis of the impact of each measurement type on the navigation performance can be carried out. It would allow to understand the contribution of each sensor as well as achieved redundancies.

Other interesting questions to be investigated are the impact of deviations from the nominal trajectory due to control errors on the navigation perfor-

mance, and augmenting the navigation filter to estimate the clock error and clock drift of the onboard receiver and considering the positioning error of the beacon.

References

1. Bora, L.: Ground beacons to enhance lunar landing autonomous navigation architectures. Master's thesis, Politecnico di Milano (2015). URL http://elib.dlr.de/100498/
2. Davies, J.L., Striepe, S.A.: Advances in POST2 End-to-End Descent and Landing Simulation for the ALHAT Project. AIAA-2008-6938. American Institute of Aeronautics and Astronautics (2008)
3. Durrant-Whyte, H., Bailey, T.: Simultaneous Localization and Mapping: Part I. IEEE Robotics & Automation Magazine pp. 99–108 (2006)
4. Epp, C., Smith, T., NASA, H.: Autonomous Precision Landing and Hazard Detection and Avoidance Technology (ALHAT). In: 2007 IEEE Aerospace Conference, pp. 1–7 (2007)
5. Heise, D.T.S.G., Steffes, S.R., Theil, S.: Filter design for small integrated navigator for planetary exploration. In: 61. Deutscher Luft- und Raumfahrtkongress 2012 (2012). URL http://elib.dlr.de/81142/
6. Houdou, B., the ESA NEXT Lunar Lander Team: NEXT Lunar Lander with In-Situ Science and Mobility: Phase A Mission Study, Mission Requirements Document. Internal Report NEXT-LL-MRD-ESA(HME)-0001, ESA (2008)
7. NASA: How to protect and preserve the historic and scientific value of u.s. government lunar artifacts. Tech. rep., National Aeronautics and Space Administration (2011)
8. Steffes, S.R.: Development and analysis of shefex-2 hybrid navigation system experiment. Ph.D. thesis, DLR Bremen (2013). URL http://elib.dlr.de/82946/
9. Theil, S., Bora, L.: Beacons for supporting lunar landing navigation. CEAS Space Journal (2016). URL http://elib.dlr.de/105766/
10. Theil, S., Krüger, H.: Analyse Missionen. Internal Report AT-RYNR-TN-002, DLR (2010)